

The spectroscopy and lasing of monoclinic $\text{Tm} : \text{KY}(\text{WO}_4)_2$ crystals

S N Bagaev, S M Vatnik, A P Maiorov, A A Pavlyuk,
D V Plakushchev

Abstract. The principal spectroscopic and lasing characteristics of a $\text{Tm}(15\%):\text{KY}(\text{WO}_4)_2$ crystal were investigated. The transition cross sections, the luminescence quantum yield, and the lifetime and the nonlinear depopulation coefficient of the upper active state were also determined. The slope efficiency of lasing at the 1950 nm wavelength was 45%. The feasibility of tuning in the spectral range 1850–1950 nm was demonstrated in principle.

1. Introduction

Thulium-doped laser crystals are used widely to generate coherent radiation in the 2 μm range, the mastering of which opens up effective opportunities for performing many practical tasks, including remote probing of the atmosphere and the development of medical laser technologies. The interest in laser sources based on thulium-doped crystals has increased with increase in the output power and operating lifetime of laser diodes and arrays, ensuring the effective pumping of the active medium in both longitudinal and transverse geometries.

It has been frequently noted in the literature [1–4] that the development of effective solid-state lasers based on thulium- and holmium-doped crystals is complicated by a whole series of undesirable factors, including the relatively small effective stimulated-emission cross sections, the quasi-three-level system characterised by a nonzero population of the lowest active states at room temperature, and also the occurrence of numerous up-conversion processes leading to the nonlinear depopulation of the upper active states and hence to a decrease in lasing efficiency.

Appropriate modelling of the operation of a laser source therefore acquires particular importance for the selection of its optimal design. Such modelling should be based on the corresponding rate equations, taking into account the populations and interaction of different energy levels as well as the spatial pump distribution and the laser-beam profile. Subject to various simplifying assumptions, such an approach has been implemented [3, 5, 6]; in many cases [1, 3, 7], a satisfactory agreement was achieved between the calculated and

experimental data for the dependence of the lasing thresholds and efficiencies of thulium- and holmium-doped YAG and YLF crystals on the pump-power density, the cavity parameters, and the spectroscopic characteristics of the crystals.

In order to expand the spectral lasing range into the short-wavelength region, it is of interest to investigate other thulium-doped crystal hosts. Spectroscopic and lasing investigations of the monoclinic $\text{Tm}(15\%):\text{KY}(\text{WO}_4)_2$ (and later $\text{Tm}:\text{KYW}$) laser crystals were carried out in the present study. The structures and principal properties of the crystals as well as the isostructural $\text{KGd}(\text{WO}_4)_2$ (KGW) crystals have been discussed in detail [8, 9]. The appreciable optical anisotropy of crystals of this group [10, 11] and the comparatively small stimulated Raman scattering threshold [9, 12] should be included among their most important characteristic features. In principle, this makes it possible to construct solid-state lasers with unique capabilities [13]. The high lasing efficiency of $\text{Nd}:\text{KGW}$ crystals has been demonstrated [14] for a longitudinal pump geometry and in the present study a similar result has been obtained for $\text{Tm}:\text{KYW}$ crystals.

2. Model

The four lowest energy levels of trivalent thulium are illustrated schematically on the right-hand side of Fig. 1, pumping where transitions lasing, transitions, and other excitation-energy relaxation channels are shown. The group of rate equations describing the interaction of Tm^{3+} ions in various energy states may be represented in the following form [3]:

$$\frac{dN_4}{dt} = R_4 - k_{4212}N_4N_1 + k_{2124}N_2^2 - \frac{N_4}{\tau_4}, \quad (1)$$

$$\frac{dN_3}{dt} = k_{2123}N_2^2 + \beta_{43} \frac{N_4}{\tau_4} - \frac{N_3}{\tau_3}, \quad (2)$$

$$\begin{aligned} \frac{dN_2}{dt} = & 2k_{4212}N_4N_1 - 2(k_{2123} + k_{2124})N_2^2 \\ & + \beta_{42} \frac{N_4}{\tau_4} + \beta_{32} \frac{N_3}{\tau_3} - \frac{N_2}{\tau_2}, \end{aligned} \quad (3)$$

$$N_1 = N_{\text{Tm}} - \sum_{i=2}^4 N_i, \quad (4)$$

where N_{Tm} is the thulium dopant concentration; the numbering of all the energy levels and kinetic constants for the pair interaction of the ions is identical with the designations in Ref. [3] (see also Fig. 1b).

S N Bagaev, S M Vatnik, A P Maiorov, D V Plakushchev Institute of Laser Physics, Siberian Division of the Russian Academy of Sciences, prospekt akad. Lavrent'eva 13/3, 630090 Novosibirsk, Russia
A A Pavlyuk Institute of Inorganic Chemistry, Siberian Division of the Russian Academy of Sciences

Received 26 November 1999

Kvantovaya Elektronika 30 (4) 310–314 (2000)

Translated by A K Grzybowski

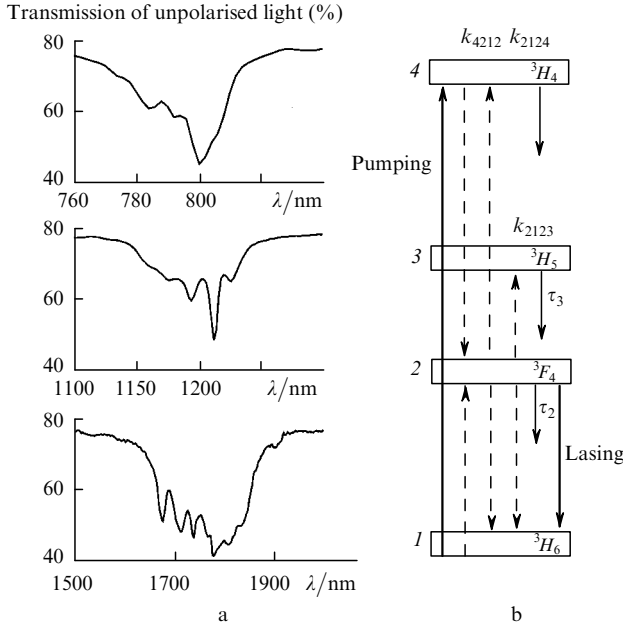


Figure 1. Transmission spectra of a Tm:KYW plate 0.92 mm thick (a) and schematic illustration of the four lowest Tm³⁺ levels and of the main energy relaxation channels (the cross-relaxation and up-conversion processes are indicated by dashed lines) (b).

In the case of a fairly short pump pulse, the effect of which reduces to an abrupt increase in the concentration of Tm³⁺ ions on level 4, the evolution of the populations of levels 2, 3, and 4 in the limit corresponding to a small density of excitations ($kN_2^2 \approx 0$) is described by a system of linear equations, the solution of which can be readily expressed as the sum of exponential terms:

$$N_i(t) = \sum_{j=2}^4 N_{ij} \exp(-A_j t), \quad i = 2, 3, 4, \quad (5)$$

where

$$A_4 = k_{4212}N_1 + 1/\tau_4; \quad A_3 = 1/\tau_3; \quad A_2 = 1/\tau_2; \quad (6)$$

the constants N_{ij} are determined from the initial conditions $N_{2,3}(0) = 0$. At fairly high thulium concentrations, when cross-relaxation is the dominant mechanism of the depopulation of level 4, expression (5) can be readily transformed into

$$N_2(t) \propto \exp(-A_2 t) - \exp(-A_4 t). \quad (7)$$

In the case of repetitively pulsed pumping, when the exciting pulses are repeated at time intervals t_0 , all the exponential terms in expressions (5) and (7) acquire additional multipliers arising on summation over preceding pulses. The following change must therefore be carried out in the above formulas:

$$\exp(-A_i t) \rightarrow \frac{\exp(-A_i t)}{1 - \exp(-A_i t_0)}. \quad (8)$$

Since Eqns (1)–(4) have been studied in detail [3] for the cw and quasi-cw operation, we believe it useful to quote only a brief compilation of the fundamental relationships necessary for the subsequent consideration of the experimental results.

The change in the pump intensity $I(z)$ is defined by the relationship

$$\frac{dI}{dz} = -\sigma_{14}(N_{\text{Tm}} - N_2)I, \quad (9)$$

where σ_{14} is the absorption cross section for the given frequency, polarisation, and direction of propagation of the beam selected as the z axis, whereas in the cw case it is defined by the expression

$$\frac{N_2}{N_{\text{Tm}}} = \frac{[(I + I_0)^2 + 2k_{\text{Tm}}II_0]^{1/2} - (I + I_0)}{2k_{\text{Tm}}I_0}. \quad (10)$$

Here

$$I_0 = \hbar\omega/A\sigma_{14}\tau_2; \quad k_{\text{Tm}} = 2N_{\text{Tm}}\tau_2(k_{2123} + Bk_{2124}); \quad (11)$$

the numerical multipliers A and B are approximately equal to two at high thulium concentrations, while their exact values were determined in Ref. [3] via the parameters of the rate equations {see Eqns (9), (10), and (21) in Ref. [3]}. Eqns (9) and (10) of our study may be integrated in terms of elementary functions; as a result, we obtain an implicit relationship $I(z)$, the comparison of which with experimental data makes it possible to determine I_0 and k_{Tm} (see Section 3).

The threshold lasing power based on the $2 \rightarrow 1$ transition may be estimated by setting the gain round-trip equal to the total cavity losses T :

$$2 \int_0^L (\sigma_{21}N_2 - \sigma_{12}N_1) dz = T, \quad (12)$$

or

$$\int_0^L N_2 dz = \frac{T + 2\sigma_{12}N_{\text{Tm}}L}{2(\sigma_{12} + \sigma_{21})} \equiv T_{\text{eff}}, \quad (13)$$

where L is the crystal length; σ_{21} and σ_{12} are the cross sections of the stimulated transition and of the absorption from the ground state at the lasing wavelength in which account has now been taken of the Boltzmann factors of the Stark-component populations of the corresponding multiplets. For the specified cavity losses T , the dependence of the right-hand side of Eqn (13) T_{eff} on the wavelength may be, generally speaking, nonmonotonic and its absolute minimum determines the range of wavelengths at which lasing will develop with the highest probability.

3. Experimental setup

Plane-parallel plates, the normal to the surfaces of which coincided with the crystallographic b axis, were prepared from a Tm:KYW single crystal grown by the low-gradient Czochralski method from a solution in the $\text{K}_2\text{W}_2\text{O}_7$ melt. The transmission spectra of the plates for the perpendicular incidence of unpolarised light were investigated on a Shimadzu spectrophotometer in the range 400–3200 nm. The luminescence spectra were measured in the standard ‘backscattering’ geometry by using a computer-controlled MDR-23U monochromator, photodetectors based on Ge:AU and PbSe, a selective UNIPAN-237 nanovoltmeter, and two analogue–digital converters, one of which was used to monitor the pump power throughout the measurements. The MDR-23U monochromator was calibrated against the emission lines of an argon laser. The absolute error and the spectral resolution for all the luminescence data presented below were estimated as 1 and 0.5 nm, respectively.

The luminescence dynamics for repetitively pulsed pumping of the crystal was recorded by a fast (1 μ s) analogue–digital converter with subsequent averaging over the results of many measurements (300–700). The crystal was pumped by a titanium–sapphire laser, which, depending on the experimental conditions, operated either in a cw regime with a Gaussian distribution of the beam profile, an output power up to 0.5 W, and an emission line width of 0.5 nm, or in a repetitively pulsed regime with a pulse repetition frequency of 183.2 Hz, a pulse duration of 1.7 μ s, and an average power up to 20 mW. The energy characteristics of the laser beams were measured by an LM-2 power meter. All the spectroscopic and lasing studies were carried out at room temperature.

Lasing based on a Tm:KYW crystal was achieved in the longitudinal pumping geometry. Single-layer antireflection coatings made of SiO₂ and ensuring a residual reflection in the range 1850–1950 nm of the order of 0.1% were deposited on both surfaces of a crystal plate 1.2 mm thick. The crystal was placed in a hemispherical cavity near a nontransmitting dichroic mirror with a transmission of 98% at the pump wavelength and a reflection of 99.8% at the lasing wavelength (Fig. 2). The output mirrors were spherical with a 37 mm radius and 3% and 20% transmission at the lasing wavelengths. The pump radiation was focused into the crystal by a quartz lens with a focal length of 100 mm. The pump intensity distribution at the lens focus was measured by a computer-controlled X–Y scanner. The distribution obtained corresponds to the typical Gaussian relationship $\exp(-r^2/\omega_0^2)$, where $\omega_0 = 55 \mu$ m.

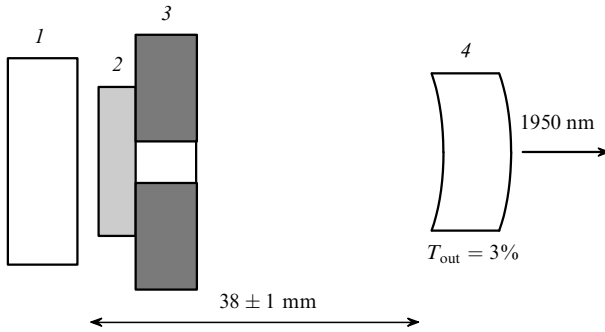


Figure 2. Design of the laser source: (1) nontransmitting mirror; (2) crystal; (3) copper heat sink; (4) output mirror.

4. Results and discussion

The absorption spectra of the Tm:KYW crystal, corresponding to transitions from the ground state to levels 2, 3, and 4, are shown in Fig. 1a. According to the data presented, radiation at a wavelength of 800 ± 1 nm is most intensely absorbed in the $1 \rightarrow 4$ transition. It pumped the crystal in all subsequent experiments. During the spectroscopic studies, only one luminescence band, corresponding to the radiative $2 \rightarrow 1$ transitions, was detected in the range 1650–2000 nm. The luminescence intensity of the $4 \rightarrow 3$ ($\sim 2.4 \mu$ m) and $3 \rightarrow 1$ ($\sim 1.2 \mu$ m) transitions was at the noise level of the measuring apparatus. The time dependence of the luminescence for repetitively pulsed pumping is illustrated in Fig. 3 by a continuous line. The dashed line constitutes its best fit by formulas (6)–(8) with the parameters $\tau_2 = 1.47$ ms and

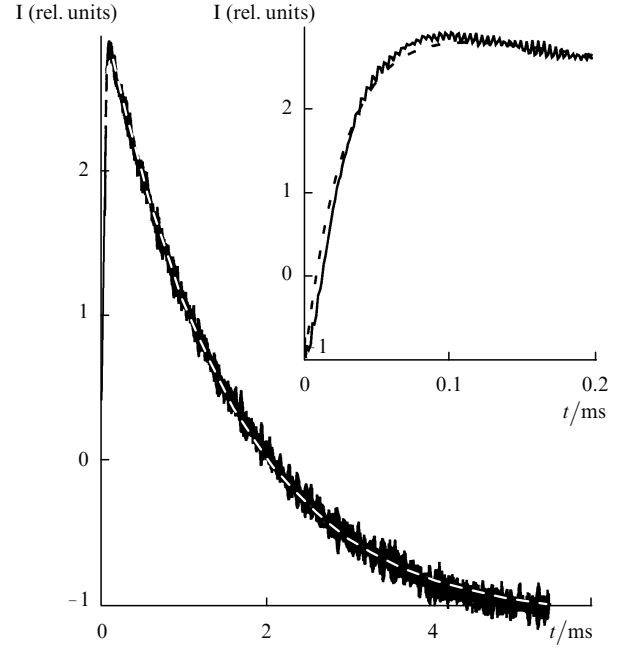


Figure 3. Dynamics of the $\lambda = 1843$ nm luminescence from the 3F_4 level with repetitively pulsed pumping and the fit to the plot by Eqns (7) and (8) (dashed curve). The inset shows the initial section of the plot.

$A_4 = 33500 \text{ s}^{-1}$. It is essential to note that, when formula (5) is fitted to the data, the minimal residual is relatively insensitive to variations in τ_3 ; taking into account the experimental errors, we are at the present time able to give only an upper estimate for τ_3 ; $\tau_3 < 30 \mu$ s.

The stimulated-transition cross section σ_{21} was determined from the luminescence measurements. On the basis of the relationships of the emission theory, discussed in detail in Ref. [15], the cross section can be easily expressed in the form

$$\sigma_{21}(\lambda) = \frac{\lambda^3 P(\lambda)}{8\pi n^2 c \tau_2^{\text{rad}} \int P(\lambda) d(Ln\lambda)}, \quad (14)$$

where λ is the wavelength; $n \approx 2$ is the refractive index of the crystal; c is the velocity of light in a vacuum; $P(\lambda)$ is the spectral density of the luminescence intensity; τ_2^{rad} is the radiative lifetime of level 2; henceforth it is assumed that the fraction of nonradiative processes is relatively small, i.e. $\tau_2^{\text{rad}} = \tau_2$. This hypothesis is based on estimates [16] and was tested experimentally in one of subsequent studies together with measurements of the temperature and concentration dependences of the kinetic coefficients in formulas (1)–(3). Fig. 4 illustrates the cross section σ_{21} , calculated according to formula (14) with corrections for the reabsorption of the luminescence, as well as the absorption cross section σ_{12} determined from the data in Fig. 1a.

Eqn (14) may be used also to estimate the radiative lifetime τ_4 of level 4. If the Boltzmann factors of the populations of levels 1 and 4 are neglected, i.e. it is assumed that the luminescence line profile for the transitions $4 \rightarrow 1$ has the same shape as the dependence of the cross section σ_{14} , on the wavelength, determined from absorption experiments, then we obtain $\tau_4 \approx 0.5$ ms for a luminescence branching ratio $\beta_{41} \approx 0.5$, which agrees quite well with the analogous quantity for a Tm:YAG crystal, i.e. $\tau_4 \approx 1$ ms.

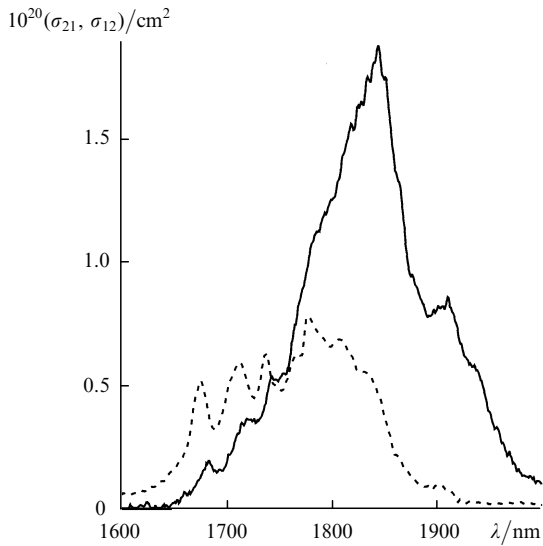


Figure 4. Cross sections σ_{21} (continuous curve) and σ_{12} (dashed curve) for a Tm:KYW crystal.

The luminescence quantum yield η , determined as the increase in the number of excitations on level 2 following the absorption of a single pump quantum, may be estimated from the values of A_4 , A_3 , and τ_4 found by using the luminescence branching ratios from Ref. [3], which affords $\eta \approx 1.90 \pm 0.07$. This result is confirmed by spectroscopic data because the estimate $\tau_4 A_4 > 20$, which yields $1.90 < \eta < 2$, can be easily obtained from a comparison of the signal/noise ratios for luminescence in the region of 2.4 μm , corresponding to the transitions $4 \rightarrow 3$, and of 1.9 μm for the transitions $2 \rightarrow 1$.

The saturation intensity $I_0 = 3300 \text{ W cm}^{-2}$ and the non-linear depopulation coefficient $k_{\text{Tm}} = 4.1$ of level 2 were determined by fitting Eqns (9)–(11) to the experimental data illustrated in Fig. 5. The multiplier A in Eqn (11) was then assumed to be 2.

According to the results of the lasing experiments presented in Fig. 6, the threshold pump power is 70 mW; with increase in pump power, the slope efficiency rose slightly

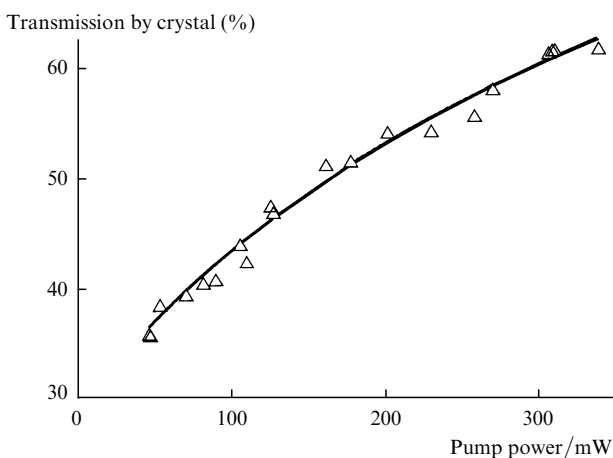


Figure 5. Dependence of the transmission by the crystal on the incident power for a focusing spot diameter of 110 μm and the beam polarisation vector directed along the optical indicatrix axis [9] [symbols — experiment, the curve was obtained by fitting Eqns (9)–(11) to this plot].

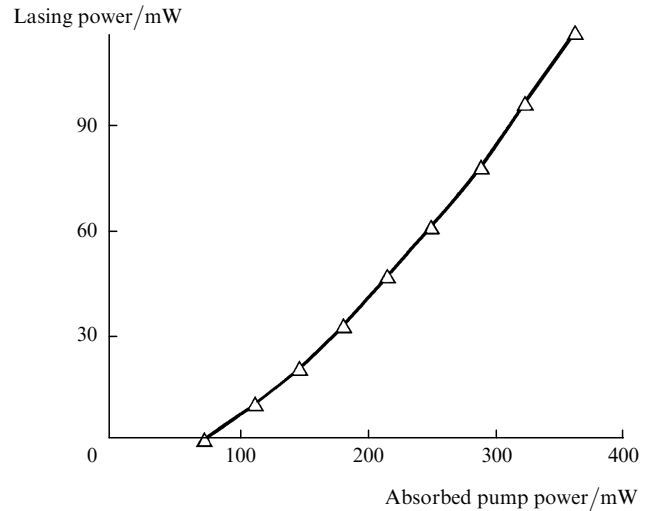


Figure 6. Dependence of the output lasing power on the absorbed pump power for a 3% transmission coefficient of the output mirror.

and reached 45% for $P_p > 200 \text{ mW}$. The pump absorption coefficient was determined from the data in Fig. 5 for the power corresponding to the lasing threshold because, on further increase in power, the populations of levels 1 and 2 do not change. Lasing was also achieved for a transmission coefficient of the output mirror of 20%; owing to the high lasing threshold, it was possible to measure only the spectral composition of the radiation, illustrated in Fig. 7 by continuous lines [the dependences of the right-hand side of Eqn (13) on the wavelength, calculated from the data in Fig. 4, are shown by dashed curves]. In full agreement with the comments to expression (13), the minima in these relationships do indeed correspond to the lasing wavelengths.

The principal spectroscopic and lasing parameters of a Tm:KYW crystal are presented in Table 1, which also lists the analogous data for a Tm(6%):YAG crystal from Ref. [3] and a Tm(12%):YAG crystal from Ref. [17]. The comparison

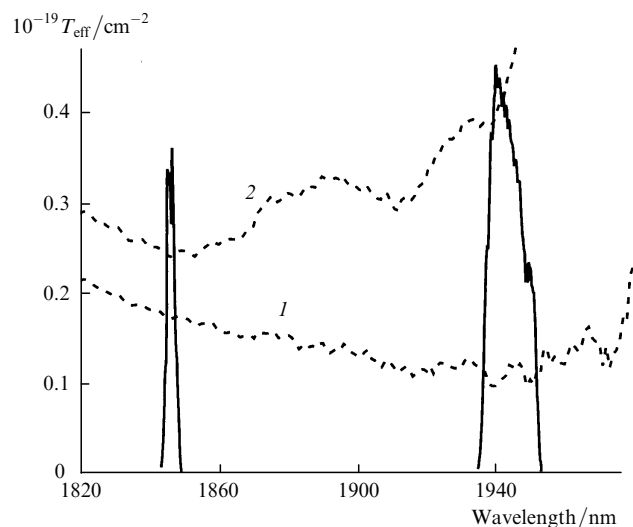


Figure 7. Spectral composition of the radiation (continuous curves) and the dependences of the right-hand side of Eqn (13) T_{eff} on the wavelength calculated from the data in Fig. 4 for $T = 3\%$ (1) and 20% (2).

Table 1.

Crystal	τ_2/ms	$10^{20}\sigma_{21}^{\text{max}}/\text{cm}^2$	$10^{18}k_{\Sigma\text{Tm}}/\text{cm}^3\text{ s}^{-1}$	$I_0/\text{W cm}^{-2}$	Lasing range/nm	Threshold pump power/mW	Slope efficiency of lasing (%)
Tm(15%): KYW	1.47	1.9	1.5	3300	1850–1950	70	45
Tm(6–12%): YAG	12 [3]	0.5 [3]	1.2–3.5 [3]	2600 [3]	1920–2130 [17]	50 [3], 200 [17]	~60 [3*, 17]

*Taking into account the intracavity losses

shows that the saturation intensities I_0 and the up-conversion coefficients $k_{\Sigma\text{Tm}}$ are virtually identical for both crystals, whereas the product $\sigma_{21}^{\text{max}}\tau_2$, which is inversely proportional to the lasing threshold, is approximately twice as great for the Tm:YAG crystal. The possible lasing tuning range for a Tm:KYW crystal (1850–1950 nm), which includes certain absorption lines of water vapour and carbon dioxide, complements satisfactorily the Tm:YAG lasing spectral range (1920–2130 nm) [17].

The slope efficiency of the lasing of a Tm:KYW crystal is presented in Table 1 without taking into account the parasitic cavity losses, which amount to 1%–1.5% according to our estimates. After appropriate corrections, this yields an efficiency of ~60%, virtually identical with the results obtained for a Tm:YAG crystal [3, 17].

5. Conclusions

The results presented permit the conclusion that, in terms of the entire set of spectroscopic and lasing characteristics, Tm:KYW crystals are promising active media for lasing in the region of ~1.9 μm . It is essential to note that the pump intensities for which lasing was achieved and investigated can be readily attained by focusing the radiation of powerful laser diodes. The relatively large pump absorption cross section with a wavelength in the region of 800 nm makes it possible to reduce the crystal thickness to a millimetre and less. This permits the construction of both microchips and tunable laser sources for the 2 μm range with an output power of hundreds of milliwatts and pumped by the radiation of laser diodes with a power of several watts.

Acknowledgements. The authors express their indebtedness to A V Kozhin and V M Tarasov for technical assistance in the preparation and carrying out of the experiments. The study was performed at the Institute of Laser Physics of the Siberian Division of the Russian Academy of Sciences with financial support by the Russian Foundation for Basic Research (Grant No. 02-97-18435).

References

- Fan T Y, Huber G, Byer R L, Mitzscherlich P IEEE J. Quantum Electron. **24** 924 (1988)
- Peterson P, Gavrielides A, Sharma P M Opt. Commun. **109** 282 (1994)
- Rustad G, Stenensen K IEEE J. Quantum Electron. **32** 1645 (1996)
- Nikitichev A A Kvantovaya Elektron. (Moscow) **15** 1462 (1988) [Sov. J. Quantum Electron. **18** 918 (1988)]
- Fan T Y, Byer R L IEEE J. Quantum Electron. **23** 605 (1987)
- Risk W P J. Opt. Soc. Am. **B 5** 1412 (1988)
- Laporta P, Brussard M IEEE J. Quantum Electron. **27** 2319 (1991)
- Kaminskii A A, Klevtsov P V, Li L, Lavluk A A Neorg. Mater. **8** 2153 (1972)
- Mochalov I V Opt. Zh. **62** (11) 4 (1995) [J. Opt. Technol. **62** 746 (1995)]
- Kaminskii A A, Sarkizov S E, Pavlyuk A A, Lyubchenko V V Neorg. Mater. **16** 720 (1980)
- Ayupov B M, Protasova V I, Pavlyuk A A, Kharchenko L Yu Neorg. Mater. **22** 1156 (1986)
- Andryunas K, Barila A, Vishchakas Yu, Mikhailov A, Mochalov I V, Petrovskii G T, Syrus I V, "Crystal active media with a high cubic nonlinearity" (Preprint) (Vilnius: Institute of Physics, 1987)
- Kaminskii A A, Ustimenko N S, Gulina A V, Bagaev S N, Pavlyuk A A Dokl. Akad. Nauk **359** 179 (1998)
- Graf T, Balmer J E Opt. Eng. (Bellingham) **34** 2349 (1995)
- Kaminskii A A Laser Crystals: Their Physics and Properties (Berlin: Springer, 1998)
- Kaminskii A A, Perlin Yu E, in Fizika i Spektroskopiya Lazernykh Kristallov (The Physics and Spectroscopy of Laser Crystals) (Moscow: Nauka, 1986), pp 125–150
- Stoneman R C, Esterowitz L Opt. Lett. **15** 486 (1990)